Yet another correlation in the analysis of CP violation using a neutrino oscillation experiment

Toshihiko Ota*
Department of Physics, Kyushu University, Hakozaki, Higashi-ku, Fukuoka 812-8581, Japan

Joe Sato†
Department of Physics, Faculty of Science, Saitama University, Saitama, 338-8570, Japan
(Received 8 November 2002; published 12 March 2003)

We investigate the effect induced by variations in the density profile of the Earth's interior using a long-baseline neutrino oscillation experiment. First, we point out two facts. (i) The most essential part of the matter profile is the first Fourier mode of the matter profile function; and (ii) the Earth models based on the study of seismology include a large uncertainty for the first Fourier mode. Next, we show that there is a strong correlation between the average density value and the first Fourier coefficient in the analysis of the oscillation probability. This means that the matter profile effect induces an added uncertainty for the average matter parameter. Taking into account this extra uncertainty, we make numerical calculations for the sensitivity to the CP violation search and show that CP sensitivity is impaired by this added uncertainty within a large U_{e3} region.

DOI: 10.1103/PhysRevD.67.053003 PACS number(s): 13.15.+g, 14.60.Lm, 14.60.Pq

I. INTRODUCTION

The effects of Earth's matter [1] play a very important role in long-baseline and high-energy oscillation experiments, such as those at a neutrino factory [2]. Furthermore, the effect of variations in matter density and chemical composition along the baseline on the oscillation probability, which we call the matter profile effect, is also a controversial issue and has been debated in various contexts [3–15].

In the search for CP-violating effects, it is important to understand the structure of the Earth so as to estimate precisely the fake signal induced by Earth's matter. Some research [13] has concluded that it is hard to obtain information about the interior of the Earth through neutrino experiments using the currently assumed size of statistics and realistic detector configurations. Therefore, the science of geophysics has been applied to support the analysis. Much analysis has used the preliminary reference Earth model (PREM) [16], an Earth model that is based on seismology. When we deal with such a model, we need to be conscious of the fact that the model includes uncertainty. In this paper, we discuss the fact that this uncertainty reduces the sensitivity to CP violation and we show that it is not a small effect.

The procedure used to demonstrate our argument is as follows. First, we recapitulate the method of the Fourier series expansion of the matter profile function [14,15] in Sec. II. Using this method, we show that only the first few modes are important in a high-energy experiment. Furthermore, we mention the uncertainty included in the seismological Earth models. We point out that a few percent error for the profile function can actually be interpreted as a huge uncertainty for the Fourier coefficients, which can affect the CP sensitivity. Next, in Sec. III, we show that there is a strong correlation between the constant matter parameter and the first Fourier coefficient of the matter profile function within a wide energy and baseline region. This fact means that the uncertainty of the matter profile effect brings added uncertainty to the average matter density. Then, we present numerical calculations to show quantitatively the loss of sensitivity induced by the uncertainty of the matter profile effect in Sec. IV. Finally, a summary is given in Sec. V.

II. METHOD OF THE FOURIER SERIES

We would like to point out two facts in this section. (1) The most essential part of the matter profile effect is the first Fourier mode of the matter profile function. (2) The seismological Earth models include great uncertainty for the first Fourier mode. These facts force us to reconsider analyses in the baseline region which have so far assumed that the matter profile effect is not significant. In the case where the baseline length is 3000 km, the PREM tells us that the matter profile function is almost flat and hence it can be expected that the matter profile effect is small. However, if we consider the uncertainty of the PREM, how will the analysis change?

A. Introduction of the method

To see the effects induced by the matter profile, we derive an analytic expression using the method of Fourier series [14,15]. Expanding the matter profile function into the Fourier modes, we obtain an extremely clear viewpoint for the resonance conditions between the oscillation lengths of the neutrino and the matter profile undulation. By this expansion we can understand which modes, and what structures, are effective.[1]

Now, we introduce our calculation method. We assume three generations and parametrize the mixing matrix of the lepton sector, the Maki-Nakagawa-Sakata-Pontecorvo matrix, as follows:

*Electronic address: toshi@higgs.phys.kyushu-u.ac.jp
†Electronic address: joe@phy.saitama-u.ac.jp

[1]The Fourier expanded-matter profile cannot reproduce the boundary between two layers precisely. However, it will be shown below that the higher modes that construct the edge are not effective in high-energy experiments.

 ©2003 The American Physical Society

$$U_{\alpha i}=\begin{pmatrix}1 & & \\ & c_\psi & s_\psi \\ & -s_\psi & c_\psi\end{pmatrix}\begin{pmatrix}1 & & \\ & 1 & \\ & & e^{i\delta}\end{pmatrix}\begin{pmatrix}c_\phi & & s_\phi \\ & 1 & \\ -s_\phi & & c_\phi\end{pmatrix}\times\begin{pmatrix}c_\omega & s_\omega & \\ -s_\omega & c_\omega & \\ & & 1\end{pmatrix}U_{\text{Majorana}}\quad(\alpha=e,\mu,\tau,\ \ i=1,2,3). \tag{1}$$

Here, s and c denote sin and cos, and U_{Majorana} is the so-called Majorana phase matrix, which does not contribute to the oscillation phenomena. The effective Hamiltonian for neutrino propagation is

$$H(x)_{\beta\alpha}=\frac{1}{2E}\left\{U_{\beta i}\begin{pmatrix}0 & & \\ & \Delta m_{21}^2 & \\ & & \Delta m_{31}^2\end{pmatrix}U_{i\alpha}^\dagger+\begin{pmatrix}a_0+\delta a(x) & & \\ & 0 & \\ & & 0\end{pmatrix}_{\beta\alpha}\right\}, \tag{2}$$

where Δm_{ij}^2 is the squared-mass difference between the ith and jth generations in a vacuum. We separate the matter effect into two parts, a_0 and $\delta a(x)$. The effect of the average matter is denoted by a_0, and $\delta a(x)$ is the matter profile part, that is, the deviation part from the average density which depends on the position x. After the separation, we expand the matter profile part into a Fourier series:

$$\delta a(x)=\sum_{\substack{n=-\infty\\ n\neq 0}}^{\infty} a_n e^{-ip_n x},\quad p_n\equiv\frac{2\pi}{L}n. \tag{3}$$

Note that the relation $a_n=a_{-n}^*$ is always satisfied because of the condition that $\delta a(x)$ is real. For the antineutrino, a_0, a_n, and δ should be replaced by $-a_0$, $-a_n$, and $-\delta$, respectively.

We treat Δm_{21}^2 and $\delta a(x)$ as perturbations and obtain the oscillation probabilities up to the first order of them, for example [15],

$$\begin{aligned}P_{\nu_e\to\nu_\mu}=&\,s_\psi^2 s_{2\tilde\phi}^2\sin^2\frac{\lambda_+-\lambda_-}{4E}L+\frac{1}{2}c_\delta s_{2\psi}s_{2\omega}s_{2\tilde\phi}\Bigg[\left(c_{\tilde\phi}c_{\phi-\tilde\phi}\frac{\Delta m_{21}^2}{\Delta m_{21}^2c_\omega^2-\lambda_-}+s_{\tilde\phi}s_{\phi-\tilde\phi}\frac{\Delta m_{21}^2}{\lambda_+-\Delta m_{21}^2c_\omega^2}\right)\\&\times\sin^2\frac{\Delta m_{21}^2c_\omega^2-\lambda_-}{4E}L-\left(c_{\tilde\phi}c_{\phi-\tilde\phi}\frac{\Delta m_{21}^2}{\Delta m_{21}^2c_\omega^2-\lambda_-}+s_{\tilde\phi}s_{\phi-\tilde\phi}\frac{\Delta m_{21}^2}{\lambda_+-\Delta m_{21}^2c_\omega^2}\right)\sin^2\frac{\lambda_+-\Delta m_{21}^2c_\omega^2}{4E}L\\&+\left(c_{\tilde\phi}c_{\phi-\tilde\phi}\frac{\Delta m_{21}^2}{\Delta m_{21}^2c_\omega^2-\lambda_-}-s_{\tilde\phi}s_{\phi-\tilde\phi}\frac{\Delta m_{21}^2}{\lambda_+-\Delta m_{21}^2c_\omega^2}\right)\sin^2\frac{\lambda_+-\lambda_-}{4E}L\Bigg]+\frac{1}{4}s_\delta s_{2\psi}s_{2\omega}s_{2\tilde\phi}\\&\times\left(c_{\tilde\phi}c_{\phi-\tilde\phi}\frac{\Delta m_{21}^2}{\Delta m_{21}^2c_\omega^2-\lambda_-}+s_{\tilde\phi}s_{\phi-\tilde\phi}\frac{\Delta m_{21}^2}{\lambda_+-\Delta m_{21}^2c_\omega^2}\right)\left(\sin\frac{\lambda_+-\Delta m_{21}^2c_\omega^2}{2E}L+\sin\frac{\Delta m_{21}^2c_\omega^2-\lambda_-}{2E}L-\sin\frac{\lambda_+-\lambda_-}{2E}L\right)\\&+4s_\psi^2s_{2\tilde\phi}^2c_{2\tilde\phi}\sum_{n=1}^{\infty}\mathrm{Re}[a_n]\frac{\lambda_+-\lambda_-}{(\lambda_+-\lambda_-)^2-(2Ep_n)^2}\sin^2\frac{\lambda_+-\lambda_-}{4E}L,\end{aligned} \tag{4}$$

$$\begin{aligned}P_{\nu_e\to\nu_\tau}=&\,c_\psi^2s_{2\tilde\phi}^2\sin^2\frac{\lambda_+-\lambda_-}{4E}L-\frac{1}{2}c_\delta s_{2\psi}s_{2\omega}s_{2\tilde\phi}\Bigg[\left(c_{\tilde\phi}c_{\phi-\tilde\phi}\frac{\Delta m_{21}^2}{\Delta m_{21}^2c_\omega^2-\lambda_-}+s_{\tilde\phi}s_{\phi-\tilde\phi}\frac{\Delta m_{21}^2}{\lambda_+-\Delta m_{21}^2c_\omega^2}\right)\sin^2\frac{\Delta m_{21}^2c_\omega^2-\lambda_-}{4E}L\\&-\left(c_{\tilde\phi}c_{\phi-\tilde\phi}\frac{\Delta m_{21}^2}{\Delta m_{21}^2c_\omega^2-\lambda_-}+s_{\tilde\phi}s_{\phi-\tilde\phi}\frac{\Delta m_{21}^2}{\lambda_+-\Delta m_{21}^2c_\omega^2}\right)\sin^2\frac{\lambda_+-\Delta m_{21}^2c_\omega^2}{4E}L+\left(c_{\tilde\phi}c_{\phi-\tilde\phi}\frac{\Delta m_{21}^2}{\Delta m_{21}^2c_\omega^2-\lambda_-}\right.\\&\left.-s_{\tilde\phi}s_{\phi-\tilde\phi}\frac{\Delta m_{21}^2}{\lambda_+-\Delta m_{21}^2c_\omega^2}\right)\sin^2\frac{\lambda_+-\lambda_-}{4E}L\Bigg]-\frac{1}{4}s_\delta s_{2\psi}s_{2\omega}s_{2\tilde\phi}\left(c_{\tilde\phi}c_{\phi-\tilde\phi}\frac{\Delta m_{21}^2}{\Delta m_{21}^2c_\omega^2-\lambda_-}+s_{\tilde\phi}s_{\phi-\tilde\phi}\frac{\Delta m_{21}^2}{\lambda_+-\Delta m_{21}^2c_\omega^2}\right)\\&\times\left(\sin\frac{\lambda_+-\Delta m_{21}^2c_\omega^2}{2E}L+\sin\frac{\Delta m_{21}^2c_\omega^2-\lambda_-}{2E}L-\sin\frac{\lambda_+-\lambda_-}{2E}L\right)\\&+4c_\psi^2s_{2\tilde\phi}^2c_{2\tilde\phi}\sum_{n=1}^{\infty}\mathrm{Re}[a_n]\frac{\lambda_+-\lambda_-}{(\lambda_+-\lambda_-)^2-(2Ep_n)^2}\sin^2\frac{\lambda_+-\lambda_-}{4E}L,\end{aligned} \tag{5}$$

$$P_{\nu_e\to\nu_e}=1-s_{2\tilde{\phi}}^2\sin^2\frac{\lambda_+-\lambda_-}{4E}L-4s_{2\tilde{\phi}}^2c_{2\tilde{\phi}}\sum_{n=1}^{\infty}\mathrm{Re}[a_n]\frac{\lambda_+-\lambda_-}{(\lambda_+-\lambda_-)^2-(2Ep_n)^2}\sin^2\frac{\lambda_+-\lambda_-}{4E}L. \tag{6}$$

We refer to the first (last) term of Eq. (4) as P^{main} ($\Sigma_{n=1}^{\infty}P_n^{\mathrm{profile}}$). Here the effective mixing angle in the average density of the matter $\tilde{\phi}$ and the squared-mass eigenvalue $\lambda_\pm$ in the average density are given by

$$\tan 2\tilde{\phi}=\frac{s_{2\phi}(\Delta m_{31}^2-\Delta m_{21}^2 s_\omega^2)}{c_{2\phi}(\Delta m_{31}^2-\Delta m_{21}^2 s_\omega^2)-a_0}, \tag{7}$$

$$\lambda_\pm=\frac{1}{2}[\Delta m_{31}^2+\Delta m_{21}^2 s_\omega^2+a_0\pm\sqrt{\{(\Delta m_{31}^2-\Delta m_{21}^2 s_\omega^2)c_{2\phi}-a_0\}^2+(\Delta m_{31}^2-\Delta m_{21}^2 s_\omega^2)^2 s_{2\phi}^2}]. \tag{8}$$

Note that the effects of the asymmetric profile do not appear in the first order of the perturbations.

The resonance conditions $\lambda_+-\lambda_-=2Ep_n$ show the energy range and width of the resonance induced by each Fourier mode. We understand that the higher Fourier mode can resonate only with the lower-energy neutrinos whose oscillation lengths are shorter [3]. Furthermore, the half-width of the amplitude becomes narrow as the mode becomes higher. This means that, if the lower-energy neutrino were to be observed precisely, the fine structure of the Earth could be known, although it is actually extremely difficult to achieve such an observation. Therefore, we conclude that only the first few Fourier modes, which are determined by the large structure of the matter profile, are relevant in the currently assumed experimental setups. This is consistent with results obtained using different methods [11–13].

B. Uncertainty of the Earth model

Knowledge of geophysics is essential since it is very difficult to ascertain the profile of the Earth from a neutrino experiment. So far, the PREM has been regarded as the absolute model. We have tended to expect that the error and the effect induced by the error are so small that they can be neglected without a careful consideration, although we have to estimate how much error the model includes in order to use the seismological Earth model. In order to discuss this error, we introduce another Earth model, ak135-f [17]. Figure 1 represents the matter profile function calculated using the PREM (solid line) and ak135-f model (dotted line) in the case where the baseline length is 3000 km and 7332 km, respectively. The profile function based on the PREM is almost flat at $L=3000$ km, and this fact guarantees that the matter profile effect is small. According to ak135-f, however, it is not so flat. If we follow this model, we may be unable to ignore the matter profile effect, even at this baseline length. Furthermore, the authors of Ref. [17] note that "the upper mantle density model should be treated with caution and may well change with further work." The upper mantle and transition area (up to 670 km in depth) occupy a large part of the path of the neutrino beam in the case of $L=3000$ km.

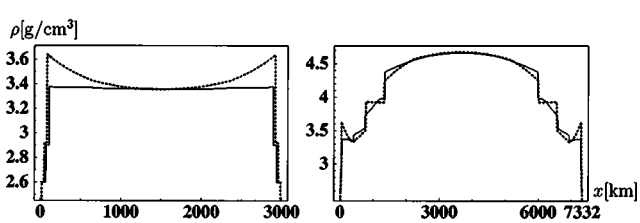

FIG. 1. The matter profile functions in the cases of 3000 km and 7332 km which are calculated using the PREM (solid line) and ak135-f (dotted line).

The baseline dependence of the average density and the first Fourier coefficient are compared in Fig. 2. These two models are different in terms of the Fourier coefficient, although they are similar with regard to the average matter density. In particular, around $L=3000$ km, the difference of the first Fourier coefficient is quite large. We need to recognize that seismological models include uncertainty, the size of which is at least equal to the difference between these two models.[2] The authors of Ref. [18] state that ± 2–3% uncertainty in the upper mantle is a reasonable estimation, which produces a large, as much as 100%, uncertainty for the first Fourier coefficient. If 2.5% error for the PREM is allowed, we can assume the matter profile depicted in Fig. 3 instead of that of the PREM itself. This profile realizes 100% shift of the first Fourier coefficient without adjusting the average matter density. We would like to stress again that the uncertainty of the average density may indeed be small, but the uncertainty of the profile is not so small that it can be neglected, especially at $L\simeq 3000$ km.

III. CORRELATION BETWEEN AVERAGE MATTER PARAMETER AND FIRST FOURIER COEFFICIENT

Here, we will establish the existence of a correlation between the parameter for the average matter density and the first Fourier coefficient of the matter profile function. The effect induced by the matter profile and its uncertainty can be understood using the concept of this correlation. Although

[2]An assumption for the profile of the underground chemical component is made when the density profile is determined in geophysics. This assumption affects the density of the electron number, which we really want to ascertain.

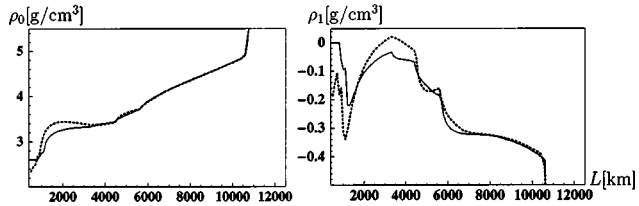

FIG. 2. The baseline dependence of the average matter density and the first Fourier coefficient which are calculated using the PREM (solid line) and ak135-f (dotted line). Around $L=3000$ km, the average densities of these two models are almost the same within a few percent, but the first Fourier coefficients differ by more than 100%.

the average density can be determined at a few percent accuracy through studies of the seismic wave and gravitational effect, etc., the matter profile effect adds extra uncertainty to the average matter density. As we pointed out in the previous section, the uncertainty of the first Fourier mode is not small, especially in the case where the neutrino beam passes mainly through the upper mantle and the transition zone, namely, where the baseline length is around 3000 km.

A. One example: $L=7332$ km

To corroborate that the correlation exists, we first present an example. In Fig. 4, the oscillation probability for $\nu_e \to \nu_\mu$ is shown where the baseline length is 7332 km. The solid line is calculated using the full PREM profile. As we showed in Ref. [15], this line is almost the same as the dash-dot-dotted line which is calculated using the up-to-first-mode profile with $\rho_0=4.2$ g/cm^3 and $\rho_1=-0.32$ g/cm^3, whose values are based on the PREM.

The dotted, dashed, and dash-dotted lines are those that are calculated using the constant-matter profile where the average density is 4.2, 4.4, and 4.6 g/cm^3, respectively. The PREM tells us that the average density in this baseline length is 4.2 g/cm^3. This figure shows that the constant profile with the average density following the PREM (dotted line) cannot reproduce the behavior of the oscillation probability with the full PREM profile (solid line). However, Fig. 4 also shows that, if a shift in the constant value is allowed, then a good fit with the full PREM calculation can be realized at $\rho_0=4.4$ g/cm^3. This fact means that the shift of the constant-matter parameter can copy the matter profile effect, which is almost equal to the effect induced by the first Fourier modes with this baseline length. We can expect that there is a strong correlation between the parameter for the average matter density and the first Fourier coefficient of the matter profile function. Indeed, this correlation is not an accidental phenomenon in this example.

We now consider the mechanism on which this correlation is based. The existence of the correlation suggests that a common shift in the average matter parameter over a wide energy region can imitate the effect of the first Fourier mode. This statement means that the relation

$$\frac{\partial P(a_n=0)}{\partial a_0}\Delta a_0=\sum_{n=1}^{\infty} P_n^{\text{profile}} \tag{9}$$

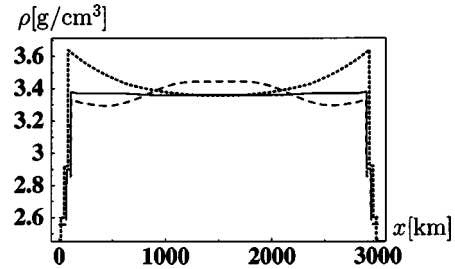

FIG. 3. An example where the deviation of the first Fourier coefficient from the PREM is more than 100% in $L=3000$ km (dashed line). This is drawn by modifying the PREM within 2.5%. The first Fourier coefficient for this profile is -0.084 g/cm^3, which is almost twice as large as that of the PREM, -0.043 g/cm^3. Solid and dotted lines are the same as those in Fig. 1.

is satisfied by a constant Δa_0 over a wide energy region. In the above example, the constant shift $\Delta\rho_0=0.2$ g/cm^3 works well within the energy region above 4 GeV. Since we can assume that the unperturbed term of the oscillation probability is dominant over the other perturbative terms and that the matter profile effect can be represented by the first mode, the condition in Eq. 9 reduces to

$$\begin{aligned}\frac{\partial P^{\text{main}}}{\partial a_0}\Delta a_0=P_1^{\text{profile}} \Leftrightarrow\ & \frac{\Delta a_0}{\lambda_+-\lambda_-}\sin\frac{\lambda_+-\lambda_-}{4E}L \\ & -\left(\frac{\Delta a_0}{4E}L\right)\cos\frac{\lambda_+-\lambda_-}{4E}L \\ & =2\left(\frac{\mathrm{Re}[a_1]}{4E}L\right)\frac{[(\lambda_+-\lambda_-)/4E]L}{\{[(\lambda_+-\lambda_-)/4E]L\}^2-\pi^2} \\ & \times\sin\frac{\lambda_+-\lambda_-}{4E}L.\end{aligned} \tag{10}$$

It is not inconsequential whether or not the constant shift Δa_0 can maintain the relation. To clarify this issue, we di-

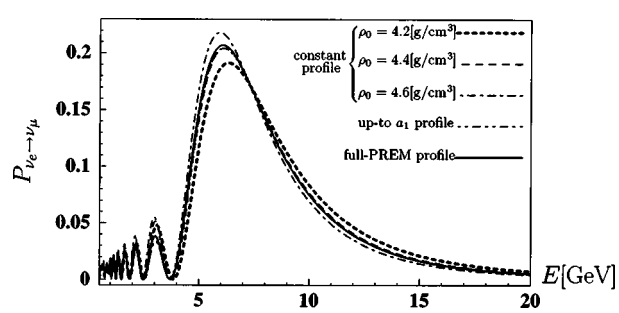

FIG. 4. Oscillation probability for $\nu_e \to \nu_\mu$ at $L=7332$ km. The dotted, dashed, and dash-dotted lines are calculated using the constant-matter profile where the values of the matter parameter are 4.2, 4.4, and 4.6 g/cm^3, respectively. The dash-dot-dotted line is calculated by the up-to-first-mode profile where the values are $\rho_0=4.2$ g/cm^3 and $\rho_1=-0.32$ g/cm^3. The solid line uses the full PREM matter profile, and this line is quite similar to the dash-dot-dotted and dashed lines. We set the oscillation parameters as $\sin\omega=0.5$, $\sin\psi=1/\sqrt{2}$, $\sin\phi=0.1$, $\Delta m_{31}^2=2.5\times10^{-3}$ eV^2, $\Delta m_{21}^2=5.0\times10^{-5}$ eV^2, and $\delta=\pi/2$.

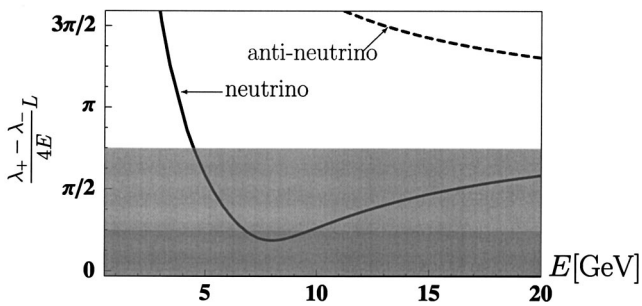

FIG. 5. Energy dependence of $(\lambda_+ - \lambda_- /4E)L$ for neutrino (solid line) and antineutrino (dashed line) at $L=$ 7332 km. The oscillation parameters used in this figure are the same as those used in Fig. 4.

vide the energy region into two regions where $[(\lambda_+ - \lambda_-)/4E]L \sim 0$ and $[(\lambda_+ - \lambda_-)/4E]L \sim \pi/2$ are satisfied, and we investigate each region.

Figure 5 shows the energy dependence of $[(\lambda_+ - \lambda_-)/4E]L$ corresponding to the case of Fig. 4. In the region of $[(\lambda_+ - \lambda_-)/4E]L \sim 0$, the condition Eq. 10 is approximated to

$$\Delta a_0 = -\frac{6}{\pi^2}\mathrm{Re}[a_1] + \mathcal{O}\left\{\left(\frac{\lambda_+ - \lambda_-}{4E}L\right)^2\right\}. \tag{11}$$

Using the value $\rho_1 = -0.32$ g/cm^3, we understand from Eq. 11 that shifting ρ_0 by 0.2 g/cm^3 makes the oscillation probability calculated with the constant profile clearly mimic the real oscillation probability, including the matter profile. Within the $[(\lambda_+ - \lambda_-)/4E]L \sim \pi/2$ region, the condition Eq. 10 is approximated by

$$\Delta a_0 = -\frac{2}{3}\mathrm{Re}[a_1] + \mathcal{O}\left(\frac{\lambda_+ - \lambda_-}{4E}L - \frac{\pi}{2}\right). \tag{12}$$

This means that the shift of a_0 so as to mimic the matter profile effect is also about 0.2 g/cm^3, which is the same as the shift in the $[(\lambda_+ - \lambda_-)/4E]L \sim 0$ region. Therefore, in a wide energy region, such as both the $[(\lambda_+ - \lambda_-)/4E]L \sim 0$ and $[(\lambda_+ - \lambda_-)/4E]L \sim \pi/2$ regions, the common shift of a_0 can indeed copy the effect of the first Fourier mode.[3]

It is an essential point for the existence of the correlation that an experiment is only sensitive to these two energy ranges.[4] We note that the condition for the antineutrino is the same as that for the neutrino. Therefore, even if the analysis is made using both neutrino and antineutrino, the correlation still exists if the observed energy region for both neutrino and anti-neutrino satisfies either $[(\lambda_+ - \lambda_-)/4E]L \sim 0$ or $[(\lambda_+ - \lambda_-)/4E]L \sim \pi/2$. In the case of $L = 7332$ km, the energy range for the antineutrino is not around either $[(\lambda_+ - \lambda_-)/4E]L \sim 0$ or $[(\lambda_+ - \lambda_-)/4E]L \sim \pi/2$, so if we could observe an adequate number of antineutrino events, the correlation would cease to hold, although the antineutrino event can be expected to be too short to be significant in a statistical sense. Therefore, we can conclude that the correlation still exists for this baseline length.

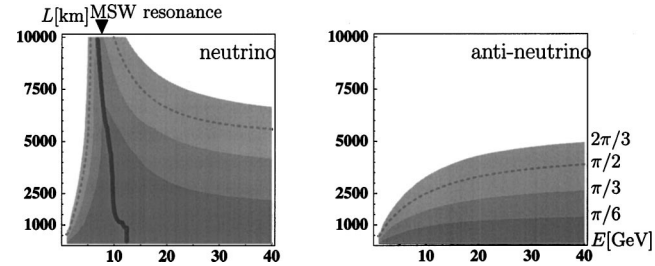

FIG. 6. Energy and baseline dependence of $[(\lambda_+ - \lambda_-)/4E]L$ for the neutrino (left plot) and antineutrino (right plot). The reference values of the parameters are the same as in Fig. 4.

B. Baseline region where the correlation exists

There is a strong correlation between a_0 and a_1 within the energy and baseline region where $[(\lambda_+ - \lambda_-)/4E]L \sim 0$, $\pi/2$ are satisfied, as we established in the previous subsection. The energy and baseline dependence of $[(\lambda_+ - \lambda_-)/4E]L$ for the neutrino and antineutrino is shown in Fig. 6. This figure tells us the region where the correlation exists. At $L \lesssim 5000$ km, $[(\lambda_+ - \lambda_-)/4E]L$ is near 0 or $\pi/2$ for both neutrino and antineutrino throughout almost all the energy range. Therefore, the common shift of a_0 for the neutrino and antineutrino can mimic the effect of a_1, that is, the correlation does exist. In the range 5000 km$\lesssim L \lesssim$7500 km, $[(\lambda_+ - \lambda_-)/4E]L$ for the antineutrino is not around either 0 or $\pi/2$. However, since there will not be a significant number of antineutrino events, in this region, the statistics will be dominated by neutrino events and hence the correlation still exists. In the region beyond 7500 km, the high-energy neutrino no longer follows the condition, and so the correlation will cease to hold. We conclude that there is a strong correlation between a_0 and a_1 in the case where the baseline length is less than 7500 km.

We would like to note one more thing. According to Eqs. 5 and 6, the same relation also holds for $\nu_e \to \nu_\tau$ and $\nu_e \to \nu_e$. So, even if we utilize these channels, the correlation will not be broken.

IV. NUMERICAL CALCULATIONS

To illustrate how the uncertainty of a_1 impairs sensitivity to CP violation, we present the numerical results for it, including the matter profile effect and its uncertainty. In an effort to clarify the difference from former research, we show simultaneously the result without consideration of the matter profile.

First, we explain briefly the procedure for drawing the sensitivity plot. We define the test statistics

[3]Moreover, we can see that this common shift works well in the intermediate region by expanding the oscillation probability around $[(\lambda_+ - \lambda_-)/4E]L \sim \pi/4$.

[4]In the region where $[(\lambda_+ - \lambda_-)/4E]L \sim \pi$ holds, the relation becomes $\Delta a_0 = -[\pi/(\pi+1)]\mathrm{Re}[a_1] + \mathcal{O}([(\lambda_+ - \lambda_-)/4E]L - \pi)$, and hence the required shift to mimic the matter profile effect is significantly different.

$$\chi^2 \equiv \min_{\substack{\text{osc. param.} \\ \delta=\{0,\pi\}}} \left[\sum_i^{\text{bin}} \frac{|\bar{N}_i^{\text{th}} \times N_i^{\text{ex}} - N_i^{\text{th}} \times \bar{N}_i^{\text{ex}}|^2}{(\bar{N}_i^{\text{th}})^2 \times N_i^{\text{ex}} + (N_i^{\text{th}})^2 \times \bar{N}_i^{\text{ex}}} \right]. \quad (13)$$

Here, N^{ex} is the "expected number of events" for $\nu_e \to \nu_\mu$ calculated using the full PREM matter profile with $\delta = \pi/2$, N^{th} is the "theoretical number of events," calculated with the constant-matter profile or the up-to-first-mode profile with $\delta = \{0,\pi\}$, and $\bar{N}$ denotes the number of events for $\bar{\nu}_e \to \bar{\nu}_\mu$. The index i stands for the energy bin. The parameters contained in N^{th} and $\bar{N}^{\text{th}}$ are varied within given ambiguities. We adjust them and minimize χ^2 to introduce the effect of the parameter correlation [2,19]. The widths of uncertainty of the parameters concerning the atmospheric and solar neutrino experiments are expected to be narrowed by near-future experiments [20]. Therefore, we assume

$$\Delta(\sin\psi) = 1\%, \quad \Delta(\Delta m_{31}^2) = 3\%,$$

$$\Delta(\sin\omega) = 5\%, \quad \Delta(\Delta m_{21}^2) = 5\%, \quad (14)$$

and for the other parameters including the matter effect we assume some options and compare them to each other. We do not deal with systematic error. We require

$$\chi^2 > \chi^2_{99\%} \quad (\text{degree of freedom} = \text{bin}) \quad (15)$$

in order to claim that the hypothesis with $\delta = \{0,\pi\}$ is excluded at the 99% level of significance, where the right-hand side is the χ^2 distribution function whose degree of freedom is the number of energy bins, not the number of parameters that fit. This is because we adopt the concept, *the power of test* (see the Appendix of Ref. [19] for more detail). The reason why we use this, less familiar, concept is that we firmly believe that we must pay attention to the fact that the best-fit point suggested by an experiment is not always located at the point chosen by nature. Remind yourself how the best-fit point for the solar neutrino deficit has changed. We actually know that there were several good-fitting regions for the solar neutrino experiments which were separated from each other on the parameter plane and which were not distributed only around the best-fit point. Moreover, the best-fit point itself moved from one region to another. To discuss the feasibility of observing some quantity with an experiment, we have to consider this fact.

We also note in passing that the degree of freedom for so-called $\Delta\chi^2$, which is often used in an estimation of the oscillation parameters, is not the number of parameters since, for example, two strongly correlated parameters are not independent of each other, and hence we should count them as one parameter. Indeed, as is commonly known, there are strong correlations for some parameters in the case we deal with.[5] We should be more careful about what is a truly measurable quantity [21], and which quantities statistics are sensitive to [19]. For instance, if the statistics can be constructed so as to be sensitive to the CP-violating effect, then there is only one parameter, Jarlskog's parameter, and the degree of freedom should be 1. Strictly speaking, only when the statistics are linearly dependent on the parameters, will the degree of freedom coincide with the number of parameters.

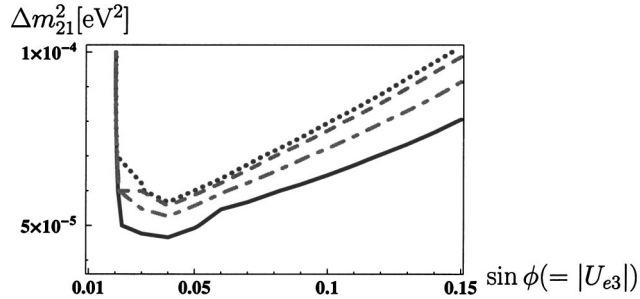

FIG. 7. Sensitivity reach for CP violation with $\delta = \pi/2$, a baseline length of 3000 km, and a muon energy of 30 GeV. The theoretical number of events N^{th} of the dotted curve is calculated using the up-to-first-mode profile, where the widths of the parameter uncertainty are assumed to be $\Delta(a_0) = 3\%$, $\Delta(a_1) = 200\%$, and $\sin\phi = 0$–0.16. For the other parameters, the uncertainty in Eq. 14 is assumed. The solid, dash-dotted and dashed curves are calculated using the constant-matter profile whose uncertainties are $\Delta a_0 = 0\%, 3\%$, and 5%, respectively, and the uncertainty for the other parameters is the same as for the dotted line.

To draw a sensitivity plot, we assume a 40 kt detector and 10^{21} muon decays in the neutrino factory scheme, and interpret Eq. 15 as the condition for Δm_{21}^2 and $\sin\phi$. Figure 7 indicates the lower boundary of Δm_{21}^2 and $|U_{e3}|$ $(=\sin\phi)$ to reject the hypotheses that δ is 0 and π at a 99% level of significance, when nature adopts the value $\delta = \pi/2$ in the case where the baseline length is 3000 km, the muon energy is 30 GeV, the detection threshold is 5 GeV, and the width of the energy bin is 2.5 GeV (10 bins). The reference values are the same as those in Fig. 4, except for Δm_{21}^2 and $\sin\phi$:

$$\sin\psi = 1/\sqrt{2}, \ \Delta m_{31}^2 = 2.5 \times 10^{-3}\ \text{eV}^2, \ \sin\omega = 0.5, \ \delta = \pi/2. \quad (16)$$

The dotted curve is calculated by considering the matter profile effect and its uncertainty up to the first Fourier mode in the calculation of Nth. We take 3% for a_0 and 200% for a_1 as the widths of the uncertainty. The other curves are calculated assuming a constant-matter profile with a different uncertainty for a_0. The solid, dash-dotted, and dashed curves correspond to $\Delta(a_0) =$ 0%, 3%, and 5%, respectively. In the minimization process, $\sin\phi$ in N^{th} is taken as an arbitrary value between 0 and 0.16, and the uncertainty of the other parameters is assumed, as in Eq. 14.

The dotted curve differs from the dash-dotted curve in which the same uncertainty for a_0 is assumed, but that for a_1 is not included. In contrast, it is very similar to the dashed curve whose uncertainty for a_0 is larger (5%), but where a constant matter profile is assumed. This fact can be explained by the correlation between a_0 and a_1 [Eqs. (11) and (12)]: The uncertainty of a_1 is translated into that of a_0 through the

[5]Depending on the conditions, it breaks the correlation to regard the oscillation parameters as not free ones, but as restricted. In the numerical calculation, this effect is automatically introduced by setting the widths of the uncertainty.

correlation, and this extra uncertainty gives rise to an extra absorption of the signal of the CP-violating effect. We know that the effect of the fake CP signal induced by the matter effect becomes more serious as $|U_{e3}|$ increases, so if $|U_{e3}|$ is measured just below the current boundary, we will have to take the effect induced by the density profile of the Earth more seriously.

In the case of $L=3000$ km, the determination of $\sin\phi$ and the reduction of its uncertainty do not contribute toward improving the sensitivity much, since the matter effect itself is large at this baseline length. Furthermore, lowering the detection threshold also hardly helps to improve the sensitivity because the number of events in the high-energy region is overwhelmingly greater than that in the low-energy region. If we can realize a lower detection threshold, an advantage can be gained with a shorter baseline length and a lower-energy beam.

Figure 8 shows the sensitivity in the case where the baseline length is 1000 km, the muon energy is 11 GeV, and the energy threshold is 1 GeV. In this plot, the dotted curve represents the calculation using the up-to-first-mode profile and its widths of parameter uncertainty are $\Delta(a_0)=3\%$, $\Delta(a_1)=200\%$, $\Delta(\sin\phi)=10\%$, and Eq. 14 for the others, the solid curve is calculated by assuming a constant-matter profile with $\Delta(a_0)=3\%$, and the dash-dotted curve is the same as the dotted one, except that $\sin\phi$ in N^{th} is assumed to be an arbitrary value between 0 and 0.16.

Within the large $|U_{e3}|$ region, the sensitivity is better than that in Fig. 7. Furthermore, the sensitivity of this choice is more robust against the uncertainty of the matter effect than in the case of $L=3000$ km. In contrast, although the signal of the CP violation is also small in the small $|U_{e3}|$ region, the fake CP violation effect induced by the matter effect is suppressed more strongly than the signal of the genuine CP violation, and hence adopting a longer-baseline and higher-energy option may be advantageous in the CP violation search.

This behavior does not come from the property of the statistics as defined by Eq. 13. When the uncertainty of the constant-matter parameter is assumed to be larger, the optimization, using the so-called $\Delta\chi^2$, also suggests that a shorter baseline length and lower energy is better (see, for example, Yasuda in Ref. [2]). The existence of this correlation tells us that, even though it is said that the uncertainty of the average matter density on the baseline is well estimated, this is not the entire uncertainty of the constant-matter parameter. We would like to stress that the uncertainty of the matter effect is no longer so small when we introduce the matter profile effect. Therefore, we should regard it more seriously whatever statistics we use, especially in the case where the main part of the neutrino beam path is the upper mantle and transition zone, including a large uncertainty for the density profile. We need to deal with the matter effect much more cautiously.

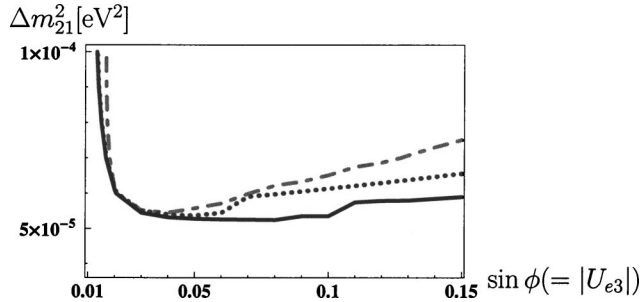

FIG. 8. Sensitivity reach for CP violation when $\delta=\pi/2$ in the case where the baseline length is 1000 km, the muon energy is 11 GeV, and the detection threshold is 1 GeV. The up-to-first-mode profile is adopted for the dotted curve where its widths of uncertainty are $\Delta(a_0)=3\%$, $\Delta(a_1)=200\%$, $\Delta(\sin\phi)=10\%$, and Eq. 14 for the other parameters. The solid curve is calculated using the constant-matter profile with $\Delta(a_0)=3\%$. By comparison with Fig. 7, it is obvious that the uncertainty of the matter effect is not serious in this situation. The dash-dotted curve is calculated in a similar manner to the dotted curve, except that $\sin\phi$ varies from 0 to 0.16. The dotted and dash-dotted curves show that the uncertainty of $\sin\phi$ will play an important role in this situation if a large $\sin\phi$ is established.

V. SUMMARY AND CONCLUSION

We pointed out that there was a very strong correlation between the constant matter parameter a_0 and the first Fourier coefficient of the matter profile function a_1, within a wide energy and baseline region. This fact means that the uncertainty of a_1 is translated into that of a_0, and this gives added uncertainty to a_0.

We also showed that there is a huge uncertainty in a_1. This is due to the fact that seismological Earth models include a large uncertainty for the density profile in the region of the upper mantle and the transition zone, which is 24–670 km in depth, and this uncertainty can cause a huge, even a few hundred percent, uncertainty for a_1. The existence of the correlation suggests that this huge uncertainty affects CP sensitivity since, due to the correlation, the uncertainty in a_1 gives added uncertainty to a_0.

We present the sensitivity plot for the CP violation effect including the matter profile effect and its uncertainty. In the case where the baseline length is 3000 km, most of the path of the neutrino beam is occupied by the upper mantle, which includes large uncertainty. We show numerically that 200% uncertainty for a_1 can be interpreted as about 2% extra uncertainty for a_0, which should be added to the original uncertainty of a_0, and this result confirms our expectations from the correlation. This extra uncertainty makes the CP sensitivity worse, especially within the large $|U_{e3}|$ region. A shorter-baseline and lower-energy option can avoid this disadvantage if the detection threshold can be lowered. On the contrary, if small $|U_{e3}|$ is established, then a long-baseline and high-energy option may be better than a shorter baseline and lower energy, because of the statistics.

We made some comments in answer to questions about the statistics that we used. We consider the fact that the best-fit parameter suggested by the experiments is not always distributed only around the parameter chosen by nature. Therefore, to discuss the feasibility of observing the CP violation

effect, we need to consider this fact. This led us to use the concept of the power of test.

In this study, we do not consider systematic uncertainty. Of course, in order to optimize the experimental configurations, it is necessary to take account of systematic error. However, in any case, we can conclude that we should regard the uncertainty of the Earth's matter as a more severe problem than has so far been assumed. We need to be much more conservative when estimating the matter effect.

ACKNOWLEDGMENTS

The authors thank the Yukawa Institute for Theoretical Physics at Kyoto University. Discussions during the YITP workshop YITP-W-02-05 on ''Flavor Mixing, *CP* Violation and Origin of Matter'' were useful for completing this work. T.O. would like to thank W. Winter for his useful comments. The work of J.S. is supported in part by Grants-in-Aid for Scientific Research from the Ministry of Education, Science, Sports, and Culture of Japan, No. 14740168, No. 14039209 and No. 14046217.

[1] L. Wolfenstein, Phys. Rev. D **17**, 2369 (1978); S.P. Mikheev and A.Yu. Smirnov, Yad. Fiz. **42**, 1441 (1985) [Sov. J. Nucl. Phys. **42**, 913 (1985)]; Nuovo Cimento Soc. Ital. Fiz., C **9**, 17 (1986); H.A. Bethe, Phys. Rev. Lett. **56**, 1305 (1986); V. Barger, K. Whisnant, S. Pakvasa, and R.J.N. Phillips, Phys. Rev. D **22**, 2718 (1980).

[2] For example, NuFact'02 Conference, http://www.hep.ph.ic.ac.uk/NuFact02/; J. Burguet-Castell, M.B. Gavela, J.J. Gomez-Cadenas, P. Hernandez, and O. Mena, Nucl. Phys. **B646**, 301 (2002); P. Zucchelli, Phys. Lett. B **532**, 166 (2002); A. Donini, D. Meloni, and P. Migliozzi, Nucl. Phys. **B646**, 321 (2002); P. Huber, M. Lindner, and W. Winter, *ibid.* **B645**, 3 (2002); O. Yasuda, hep-ph/0209127; hep-ph/0203273; for a reference list, see T. Ota, J. Sato, and N. Yamashita, Phys. Rev. D **65**, 093015 (2002).

[3] P.I. Krastev and A. Yu. Smirnov, Phys. Lett. B **226**, 341 (1989).

[4] P.I. Krastev and S.T. Petcov, Phys. Lett. B **205**, 84 (1988); S.T. Petcov, *ibid.* **434**, 321 (1998); M.V. Chizhov and S.T. Petcov, Phys. Rev. D **63**, 073003 (2001); Phys. Rev. Lett. **83**, 1096 (1999); J. Bernabeu, S. Palomares-Ruiz, A. Perez, and S.T. Petcov, Phys. Lett. B **531**, 90 (2002).

[5] E.K. Akhmedov, Nucl. Phys. **B538**, 25 (1999); Pramana **54**, 47 (2000); Yad. Fiz. **64**, 851 (2001) [Phys. At. Nucl. **64**, 787 (2001)]; E.K. Akhmedov, A. Dighe, P. Lipari, and A.Y. Smirnov, Nucl. Phys. **B542**, 3 (1999).

[6] M. Freund and T. Ohlsson, Mod. Phys. Lett. A **15**, 867 (2000); T. Ohlsson and H. Snellman, J. Math. Phys. **41**, 2768 (2000); **42**, 2345(E) (2001); Phys. Lett. B **474**, 153 (2000); T. Ohlsson, *ibid.* **522**, 280 (2001).

[7] I. Mocioiu and R. Shrock, Phys. Rev. D **62**, 053017 (2000).

[8] G.L. Fogli, G. Lettera, and E. Lisi, hep-ph/0112241.

[9] E.K. Akhmedov, P. Huber, M. Lindner, and T. Ohlsson, Nucl. Phys. **B608**, 394 (2001).

[10] T. Miura, E. Takasugi, Y. Kuno, and M. Yoshimura, Phys. Rev. D **64**, 013002 (2001); T. Miura, T. Shindou, E. Takasugi, and M. Yoshimura, *ibid.* **64**, 073017 (2001).

[11] L. Shan, B. Young, and X. Zhang, Phys. Rev. D **66**, 053012 (2002).

[12] B. Jacobsson, T. Ohlsson, H. Snellman, and W. Winter, Phys. Lett. B **532**, 259 (2002).

[13] T. Ohlsson and W. Winter, Phys. Lett. B **512**, 357 (2001); M. Lindner, T. Ohlsson, R. Tomas, and W. Winter, hep-ph/0207238.

[14] M. Koike and J. Sato, Mod. Phys. Lett. A **14**, 1297 (1999).

[15] T. Ota and J. Sato, Phys. Rev. D **63**, 093004 (2001).

[16] A.M. Dziewonski and D.L. Anderson, Phys. Earth Planet. Inter. **25**, 297 (1981).

[17] B.L.N. Kennett, E.R. Engdahl, and R. Buland, Geophys. J. Int. **122**, 108 (1995); http://wwwrses.anu.edu.au/seismology/ak135/intro.html

[18] R. Geller and T. Hara, hep-ph/0111342.

[19] M. Koike, T. Ota, and J. Sato, Phys. Rev. D **65**, 053015 (2002).

[20] JHF-SK Collaboration, Y. Itoh *et al.*, hep-ex/0106019; for KamLand experiment, see P. Aliani, V. Antonelli, M. Picariello, and E. Torrente-Lujan, hep-ph/0207348; M.C. Gonzalez-Garcia and C. Pena-Garay, Phys. Lett. B **527**, 199 (2002); H. Murayama, Phys. Rev. D **65**, 013012 (2002); V.D. Barger, D. Marfatia, and B.P. Wood, Phys. Lett. B **498**, 53 (2001).

[21] J. Sato, Nucl. Instrum. Methods Phys. Res. A **472**, 434 (2001).